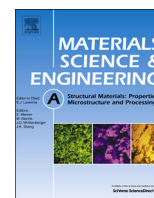




ELSEVIER

Contents lists available at ScienceDirect

## Materials Science &amp; Engineering A

journal homepage: [www.elsevier.com/locate/msea](http://www.elsevier.com/locate/msea)

## Aging behavior and precipitates analysis of the Cu–Cr–Zr–Ce alloy

Yi Zhang<sup>a,b,d,\*</sup>, Alex A. Volinsky<sup>b,\*</sup>, Hai T. Tran<sup>b</sup>, Zhe Chai<sup>a,c</sup>, Ping Liu<sup>c</sup>, Baohong Tian<sup>a,d</sup>, Yong Liu<sup>a,d</sup><sup>a</sup> College of Materials Science and Engineering, Henan University of Science and Technology, Luoyang 471003, China<sup>b</sup> Department of Mechanical Engineering, University of South Florida, Tampa 33620, USA<sup>c</sup> College of Materials Science and Engineering, University of Shanghai for Science and Technology, Shanghai 200093, China<sup>d</sup> Collaborative Innovation Center of Nonferrous Metals, Luoyang, Henan Province 471003, China

## ARTICLE INFO

## Article history:

Received 5 August 2015

Received in revised form

12 October 2015

Accepted 13 October 2015

## Keywords:

Cu–Cr–Zr–Ce alloy

Cold rolling

Aging treatment

Microstructure

Physical properties

## ABSTRACT

Microstructure of the Cu–Cr–Zr–Ce alloy was investigated by high resolution transmission electron microscopy (HRTEM), along with micro-hardness and electrical conductivity measurements. The alloy hardness and electrical conductivity can reach 170 HV and 66% IACS, respectively, after 80% cold rolling and aging for 16 h at 300 °C. Under the same aging conditions, without cold rolling, the hardness is 90 HV and electrical conductivity is 44% IACS. Two kinds of Cr and Cu<sub>4</sub>Zr precipitates were identified by TEM characterization after aging at 400 °C for 8 h. HRTEM microstructure analysis shows the presence of chromium-rich particles after aging for 18 h at 300 °C. Precipitates with ordered fcc structure are coherent with the matrix. Most of the precipitates are club-shaped chromium-rich particles, around 10–15 nm in size. The phase transformation kinetics was determined during aging. This study explored optimized processing conditions of the Cu–Cr–Zr–Ce alloy.

© 2015 Elsevier B.V. All rights reserved.

## 1. Introduction

Copper alloys are widely used in electronics because of good electrical conductivity and high strength [1–4]. Electronic packaging lead frame is one of the main parts of an integrated circuit. The function of the lead frame is to provide channels for electronic signals between devices and circuits, and fixing devices on the circuit board [5–9]. Thus, the lead frame alloys are required to have high strength and conductivity. The copper-based lead frame materials can be divided into three major categories: Cu–Fe–P alloys, Cu–Ni–Si alloys and Cu–Cr–Zr alloys. Cu–Cr–Zr alloy is considered to be the third generation of the lead frame material due to its high strength (> 600 MPa), high hardness (> 180 HV) and high electrical conductivity (> 80% IACS) [10–15].

In recent years, many aging processes were used to improve the strength and electrical conductivity of the Cu–Cr–Zr alloy. During the aging treatment, precipitation strengthening mechanisms make a great contribution to the strength and electrical conductivity of the alloy. Xia et al. [16] studied the hot rolled-quenched Cu–0.39Cr–0.24Zr–0.072Mg–0.021Si alloy and found that the hardness, strength, and electrical conductivity of the alloy are up to 198 HV, 567 MPa, and 77.8% IACS, achieved by the two-step cold

rolling and aging process. Mu et al. [17] have identified three kinds of precipitates to be the chromium-rich phase, the zirconium-rich phase and the Heselur phase in the Cu–0.43Cr–0.17Zr–0.05Mg–0.1RE alloy. Pan et al. [18] found Cr and Cu<sub>5</sub>Zr by studying the Cu–0.81Cr–0.12Zr–0.05Y–0.05La alloy. Liu et al. [19] found the Heselur phase, CrCu<sub>2</sub>(Zr,Mg) and Cu<sub>4</sub>Zr at the grain boundaries after studying the Cu–0.6Cr–0.15Zr–0.05Mg alloy by rapid solidification. Su et al. [20] also found similar results by studying the Cu–0.7Cr–0.13Zr alloy. However, there has been no unanimous agreement on the phase transformation and strengthening mechanisms of the Cu–Cr–Zr alloys. Almost all studies used the aging temperature of more than 400 °C. Thus, it is necessary to study the phase transformation and strengthening mechanisms of the Cu–Cr–Zr alloys aging at 400 °C.

In this study, Cu–Cr–Zr alloy containing Ce was investigated. The microstructure and physical properties of the Cu–Cr–Zr–Ce alloy were investigated. In addition, the influence of the aging processes on the strengthening particles was discussed in relation with the phase transformation mechanisms.

## 2. Experimental details

The experimental alloy was melted in a vacuum induction furnace under argon atmosphere using cathode copper, pure chromium, pure spongy zirconium and pure cerium, and then cast into a low carbon steel mold with  $\Phi$  83 mm  $\times$  150 mm dimensions. Its

\* Corresponding authors.

E-mail addresses: [zhshgu436@163.com](mailto:zhshgu436@163.com) (Y. Zhang), [volinsky@usf.edu](mailto:volinsky@usf.edu) (A.A. Volinsky).

chemical composition in wt% is: 0.4Cr, 0.15Zr, 0.05Ce and Cu balance. The ingot was homogenized at 930 °C for 2 h to remove the alloying elements segregation. Subsequently, the ingot was forged into bars 25 mm in diameter. The forged bars were solution-treated at 900 °C for 1 h, followed by water quenching. The alloy was cold rolled with 40%, 60%, or 80% reduction, respectively. The aging treatments were carried out in a tube electric resistance furnace in argon with  $\pm 5$  °C temperature accuracy. The aging temperature and time were ranged from 250 °C to 400 °C and 2 h to 24 h, respectively. The microhardness was measured using a HVS-1000 hardness tester with 200 g load and 5 s holding time. Electrical resistance was measured using the ZY9987 micro-ohmmeter. Microstructure was investigated using OLYMPUS PMG3 metallographic microscope. Samples for transmission electron microscopy (TEM) characterization were prepared using Gatan 691 Ion Beam Thinner. The precipitated phase was identified by the JEM-2100 high resolution transmission electron microscope (HRTEM).

### 3. Results and discussion

#### 3.1. Physical properties

The variation in hardness of the alloy aged at 250 °C, 300 °C, 350 °C and 400 °C after 80% cold rolling reduction is shown in Fig. 1(a). It can be seen that the hardness of the alloy aged at 350 °C and 400 °C increases quickly initially and then slowly with the aging time. The cold-rolled alloy shows a peak hardness of 183 HV after an aging time of 6 h at 400 °C and 172 HV after an aging time of 10 h at 350 °C, respectively. The higher the aging temperature, the faster the solute diffusion and therefore the shorter the time to reach the maximum hardness. It was shown that the hardness decreased first and then increased with aging time under the aging temperature of 300 °C. This is because the aging temperature was too low, so the precipitation rate of the secondary phase was too slow. The secondary phase precipitation strengthening was weaker than the softening effect from heating. After that, the hardness of the alloy increased slowly.

The curves of the conductivity of the alloys aged at 250 °C, 300 °C, 350 °C and 400 °C are shown in Fig. 1(b). At the beginning of aging electrical conductivity increased rapidly, but the time for reaching the peak conductivity is different for the alloy aged at different temperature. The higher the aging temperature, the shorter the time for reaching the peak conductivity. The conductivity can reach 83% IACS for the alloy aged at 400 °C for 2 h. This is due to the solute elements precipitating out of the supersaturated solution. As aging time increases further, conductivity reaches a stable value and then increases slightly as the solute concentration in copper approaches equilibrium. The aging temperature of 250 °C was too low and the conductivity did not change much.

Fig. 2 shows variations in hardness and conductivity for the Cu–Cr–Zr–Ce alloy aged at 300 °C. With increasing cold rolling reduction the Cu–Cr–Zr–Ce alloy hardness increased in Fig. 2(a). The hardness of the alloy with 80% cold rolling aged for 16 h at 300 °C increased to a maximum value of 170 HV and then decreased. Under the same aging conditions without cold rolling, the hardness is only 90 HV. Dislocations resulting from cold rolling act as diffusion paths for solute atoms and provide nucleation sites for precipitation during aging treatment [21].

The alloy conductivity increased after aging with cold rolling reduction in Fig. 2(b). With 40%, 60% and 80% cold rolling reduction, the alloy conductivity reached 60%, 63% and 66% IACS when aged at 300 °C for 16 h, respectively. Under the same aging conditions with no deformation, electrical conductivity is only 44% IACS. The conductivity had a slow increase up to 16 h of aging and

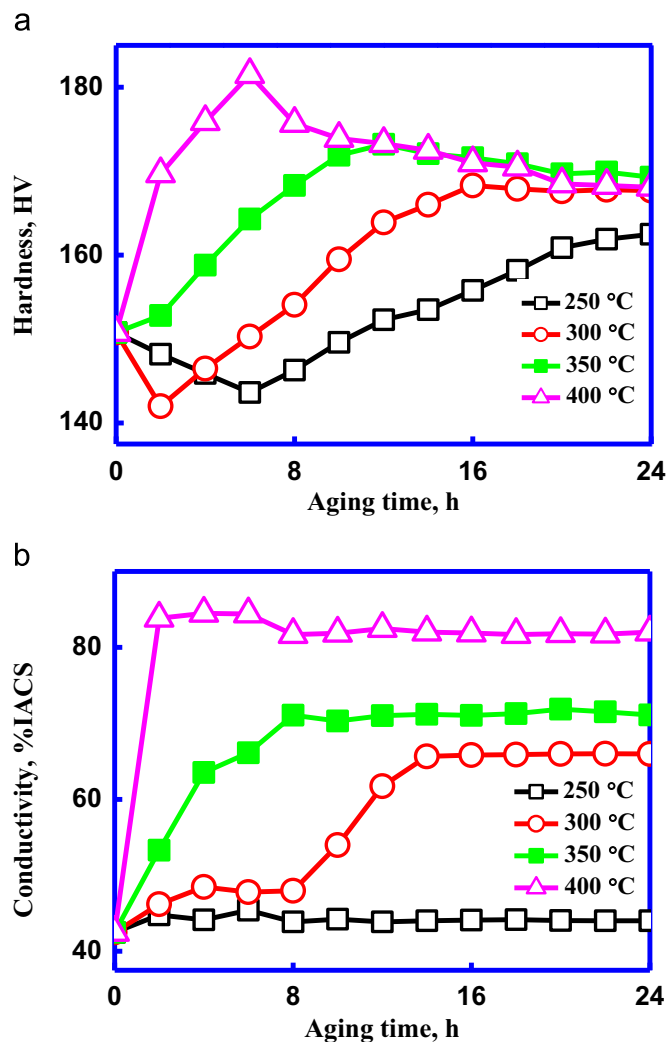


Fig. 1. Aging temperature effect on: (a) the hardness and (b) conductivity of the 80% cold rolled Cu–Cr–Zr–Ce alloy.

then became nearly constant with further increase in aging time, up to 24 h.

#### 3.2. Microstructure characterization

Fig. 3 shows TEM images of the Cu–Cr–Zr–Ce alloy cold rolled 60% and aged at 300 °C for 2 h. High dislocation density is introduced and dislocation tangles are formed by heavy cold rolling in Fig. 3(a). Grains of the secondary phases are found in the Cu matrix and along the grain boundaries in Fig. 3(b). These dispersed particles provide resistance to the motion of dislocations. Annealing twins were observed after recovery of the deformed grains. Dislocation density decreased in the grains. It can be seen in Fig. 2(a) that the hardness of the alloy cold rolled by 60% decreased after aging at 300 °C for 2 h.

Fig. 4 shows TEM images of the Cu–Cr–Zr–Ce alloy cold rolled 80% and aged at 350 °C for 4 h and 8 h. It can be seen that small and well dispersed particles precipitate in the Cu matrix. With the increase of the aging time, more precipitates were observed in Fig. 4(b). Cold rolling of the alloy results in a high density of dislocations and deformation bands, which depend on the degree of deformation. Dislocations and deformation bands generated during cold rolling act as nucleation sites for further precipitation during aging treatment [22]. High dislocation density provides a large number of nucleation sites and therefore faster rate of

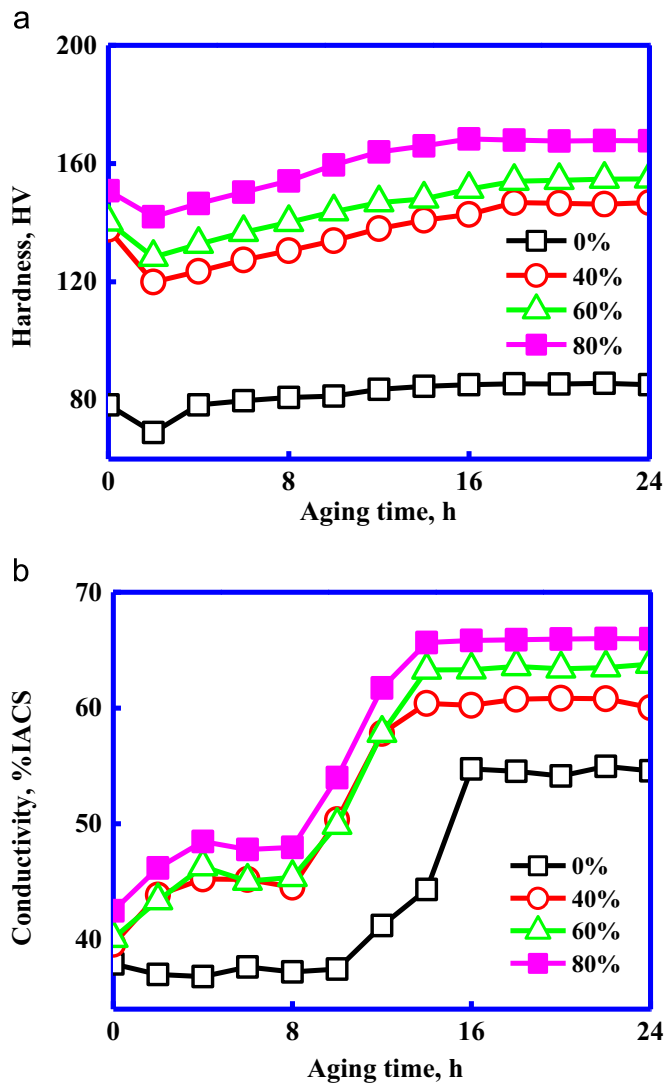


Fig. 2. Cold deformation effect on: (a) the hardness and (b) conductivity of the Cu–Cr–Zr–Ce alloy aged at 300 °C.

precipitation and growth. Therefore, more precipitates were observed in Fig. 4 than in Fig. 3.

TEM images with corresponding selected area electron diffraction (SAED) pattern of the Cu–Cr–Zr–Ce alloy cold rolled at 80% and aged at 400 °C for 4 h and 8 h are shown in Fig. 5. Compared with Fig. 4, a large number of small and well dispersed particles precipitated in the Cu matrix at the same aging time. Two kinds of Cr and  $\text{Cu}_4\text{Zr}$  precipitates were identified by TEM characterization after aging for 8 h at 400 °C. It appears that these precipitates can act as obstacles to prevent dislocation movement during cold rolling. As a result, the alloy was strongly strengthened compared with aging at 350 °C. Therefore, higher hardness was obtained with aging at 400 °C compared with 350 °C, as shown in Fig. 1(a). The precipitation hardening effect is strongly dependent on the size and distribution of precipitates. According to Fig. 5(b), the coarsening of precipitates was observed after aging for 8 h at 400 °C. Thus, it can be seen that the hardness decreased with the aging time in Fig. 1(a). Due to precipitation and coarsening of precipitates from the Cu matrix, the increase in conductivity was attributed to the decrease in the scattering surfaces for the conducting electrons. Thus, the conductivity increased with the aging temperature in Fig. 1(b).

TEM and HRTEM micrographs, along with the corresponding selected area electron diffraction (SAED) pattern are shown in Fig. 6(a)–(c), respectively. Fig. 6(a) shows that a large amount of particles had precipitated in the Cu matrix during aging. To investigate the precipitates dispersed in the matrix, HRTEM was used to examine the shape of the precipitates aged at 300 °C for 18 h after cold rolling. Precipitates are coherent with the matrix. Most of the precipitates are club-shaped chromium-rich particles, around 10–15 nm in size. Selected area diffraction patterns obtained from the precipitate are shown in Fig. 6c. Precipitates have a structure corresponding to the fcc chromium-rich phase. This is in agreement with the previous results, where ordered fcc precipitates were considered to be precursors for the chromium-rich ordered bcc precipitates formation [8]. However, there are many different opinions about the types of precipitates in the Cu–Cr–Zr alloy. Other research results concluded that the precipitates were Cr,  $\text{Cu}_4\text{Zr}$ ,  $\text{CrCu}_2$ ,  $\text{Cu}_5\text{Zr}$  and so on [16,17,19,20]. This may be because the temperature in previous investigations was more than 400 °C, while in the present study initial precipitation stage is under 400 °C. Small additions of Ce can have beneficial effects on

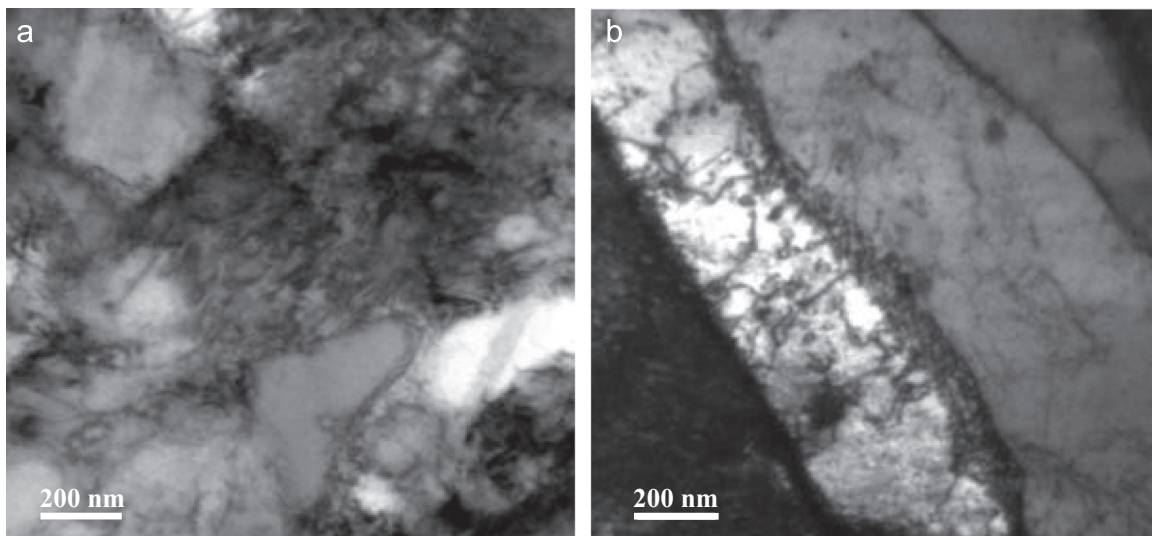
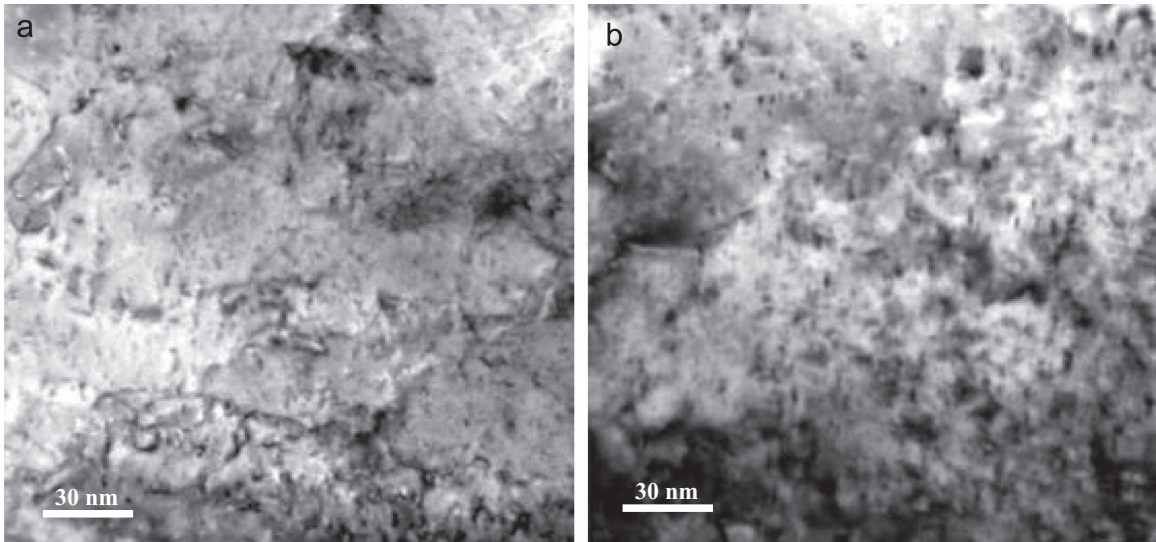
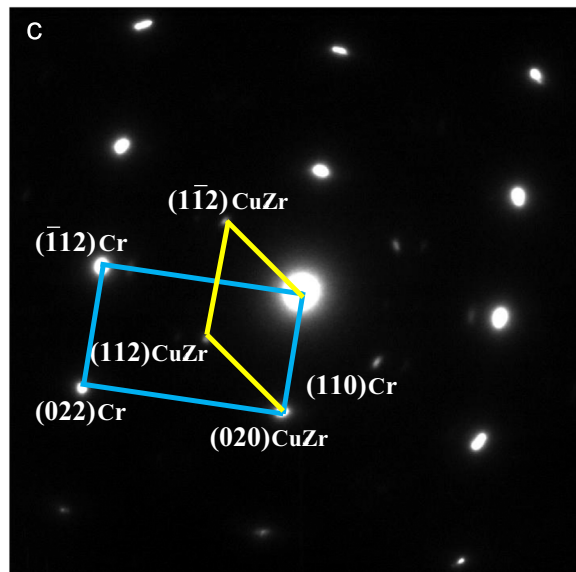
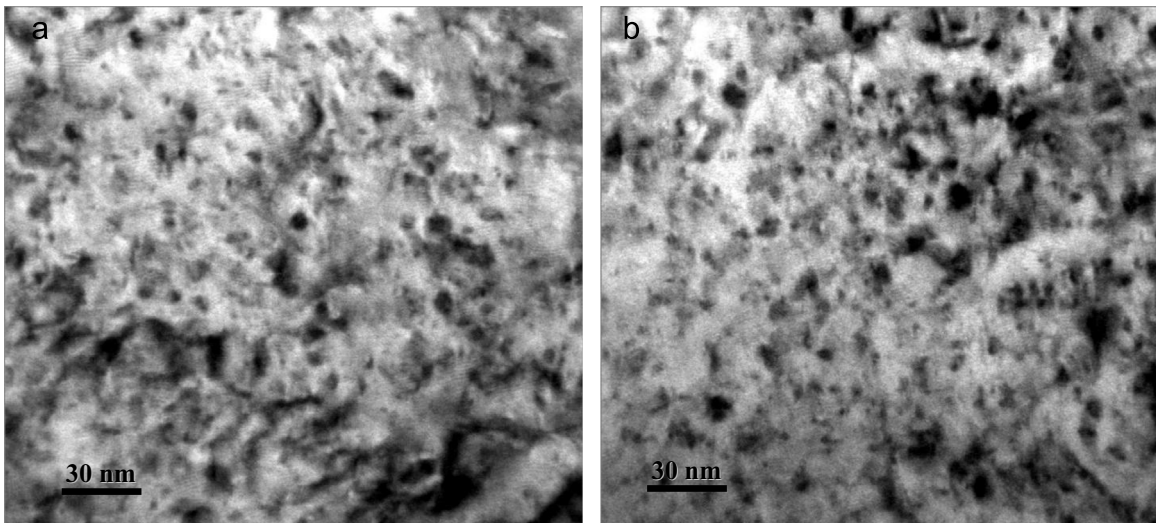


Fig. 3. TEM images of the Cu–Cr–Zr–Ce alloy after 60% cold rolling and 300 °C aging for 2 h.



**Fig. 4.** TEM images of the Cu–Cr–Zr–Ce alloy after 80% cold rolling and 350 °C aging for: (a) 4 h and (b) 8 h.



**Fig. 5.** TEM images and SAED patterns of Cu–Cr–Zr–Ce alloy after 80% cold rolling and 400 °C aging for 4 h (a), 8 h (b) and (c) SAED pattern for (b).

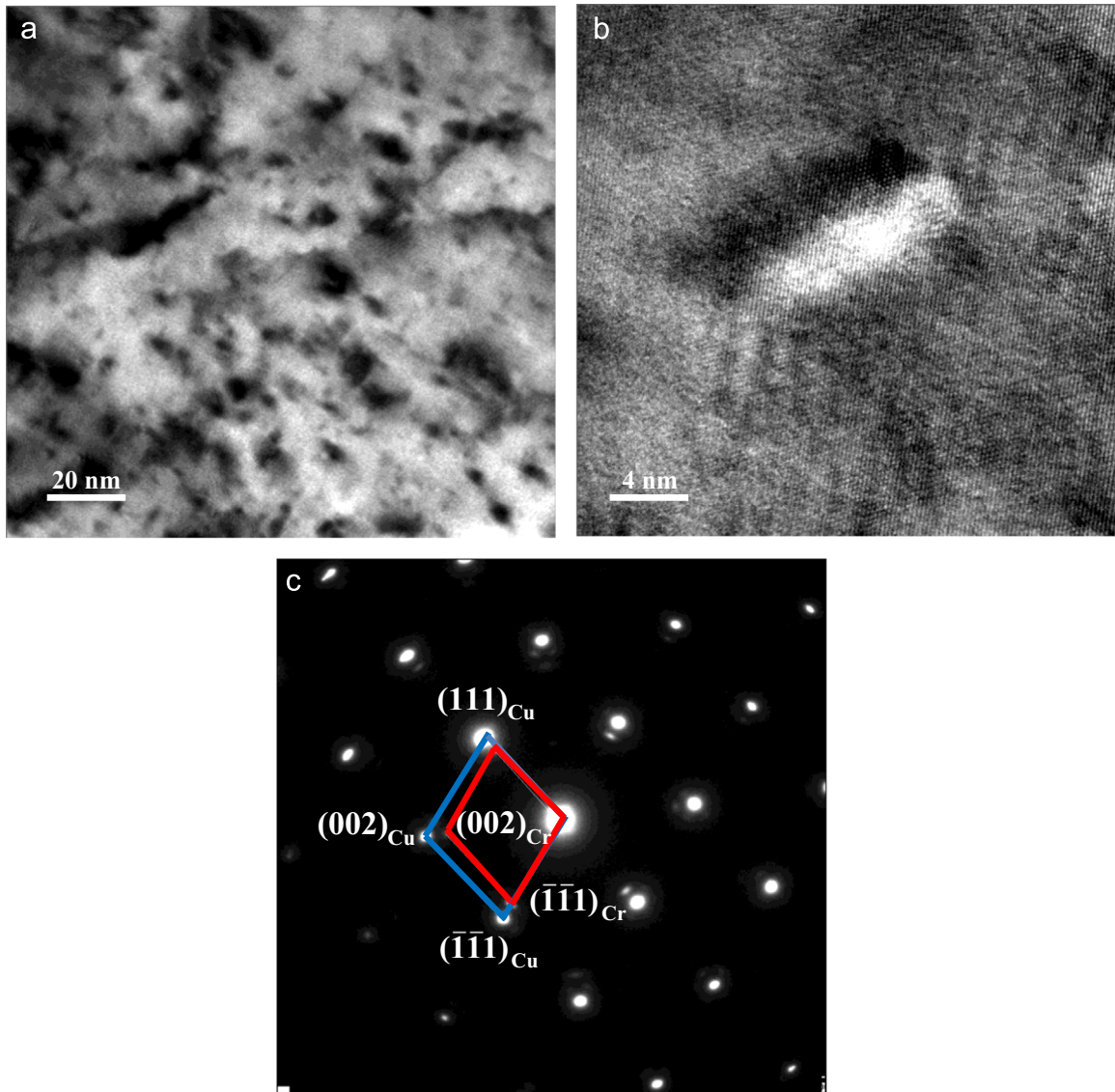


Fig. 6. TEM micrographs and SAED pattern of the alloy aged at 300 °C for 18 h: (a) substructure; (b) HRTEM micrograph of the precipitates; (c) SAED pattern from (a).

the Cu–Cr alloy properties. The additions may clean the grain boundary and increase the nucleation rate of the precipitates [23,24]. However, investigators could not reach an agreement about the effects of Ce because no fine precipitates with Ce have been explicitly observed during aging.

### 3.3. Phase transformation kinetics equation

The phase transformation of this alloy can be investigated through the variations of electrical conductivity during aging. The volume fraction of phase transformation can be expressed as [25]:

$$f = V/V_c \quad (1)$$

here,  $V_c$  is the equilibrium volume of new precipitates in a unit volume of the matrix at the end of precipitation.  $V$  stands for the volume of new precipitates formed in a unit volume of the matrix for a certain time. Before phase transformation,  $V=0$  and  $f=0$ . After a long aging time, the electrical conductivity can hardly increase, so  $V=V_c$  and  $f=1$ . According to the Matthesen's rule, the electrical conductivity and volume fraction of precipitates has a linear relationship, which can be expressed as:

$$\sigma = \sigma_0 + (\sigma_{\max} - \sigma_0)f \quad (2)$$

According to Eq. (2),  $f = (\sigma - \sigma_0)/(\sigma_{\max} - \sigma_0)$ . Thus,  $f$  can be calculated at any aging temperature. The kinetics Avrami equation of phase transformation can be expressed as [26]:

$$f = 1 - \exp(-bt^n) \quad (3)$$

here,  $f$  is the volume fraction of the transformed phase;  $b$  and  $n$  are constants and  $t$  is aging time. Taking natural logarithms of both sides of Eq. (3):

$$\log [\ln(1/(1-f))] = \log b + n \log t \quad (4)$$

The relationship between  $\lg [\ln(1/(1-f))]$  and  $\log t$  is shown in Fig. 7. Here,  $n$  is the slope of the line and  $\log b$  is the intercept. Therefore, the phase transformation kinetics equation of the Cu–Cr–Zr–Ag alloy cold rolled by 80% and aged at 300 °C, 350 °C and 400 °C can be expressed as:

$$300 \text{ } ^\circ\text{C} \quad \sigma = 42.48 + 23.52[1 - \exp(-0.004t^{2.4})] \quad (5)$$

$$350 \text{ } ^\circ\text{C} \quad \sigma = 42.48 + 29.36[1 - \exp(-0.25t^{1.05})] \quad (6)$$

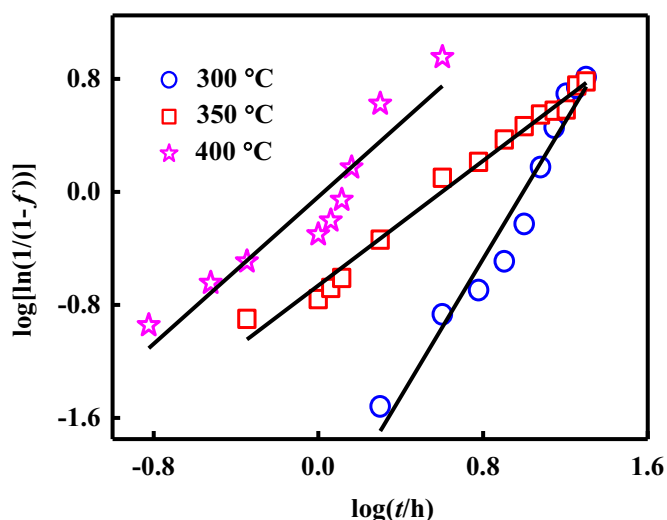


Fig. 7. Relations between  $\log[\ln(1/(1-f))]$  and  $\log t$  of Cu–Cr–Zr–Ag alloy cold rolled at 80% and aged at 300 °C, 350 °C and 400 °C.

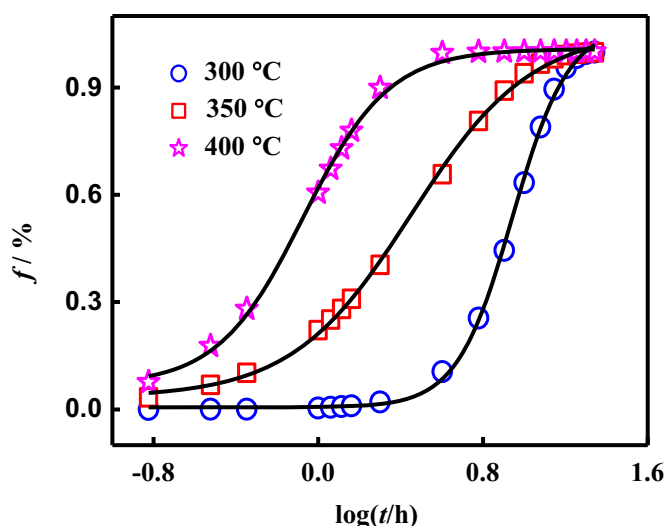


Fig. 8. Phase transformation kinetics curves of Cu–Cr–Zr–Ag alloy cold rolled 80% and aged at 300 °C, 350 °C and 400 °C.

$$400\text{ °C } \sigma = 42.48 + 41.99[1 - \exp(-0.93t^{1.3})] \quad (7)$$

The phase transformation kinetics curves are shown in Fig. 8, based on Eqs. (5)–(7). It can be seen that the experimentally obtained values are in agreement with theoretical analysis.

#### 4. Conclusions

Cold-rolled Cu–Cr–Zr–Ce alloy shows a peak hardness of 183 HV after 6 h aging at 400 °C with 80% cold rolling. Electrical conductivity can reach 83% IACS when aged at 400 °C for 2 h. Hardness and electrical conductivity can reach 170 HV and 66% IACS, respectively, after 80% cold rolling and 16 h aging at 300 °C.

Under the same aging conditions without cold rolling, hardness and electrical conductivity is 90 HV and 44% IACS, respectively. Two kinds of Cr and  $\text{Cu}_4\text{Zr}$  precipitates were identified by TEM characterization after aging at 400 °C for 8 h. Precipitates with ordered fcc structure are coherent with the matrix after aging at 300 °C for 18 h. Most of the precipitates are club-shaped chromium-rich particles, around 10–15 nm in size. The phase transformation kinetics equations of Cu–Cr–Zr–Ag alloy cold rolled at 80% and aged at 300 °C, 350 °C and 400 °C were determined during aging. This study found optimized processing conditions for the Cu–Cr–Zr–Ce alloy from the standpoint of maximum hardness and electrical conductivity for the lead frame applications.

#### Acknowledgments

This work was supported by the National Natural Science Foundation of China (51101052) and the National Science Foundation (1358088).

#### References

- [1] H.T. Tran, M.H. Shirangi, X. Pang, A.A. Volinsky, *Int. J. Fract.* 185 (2013) 115–127.
- [2] S.C. Krishna, K.V. Radhika, K.T. Tharian, M.S. Kiranmayee, G.S. Rao, A.K. Jha, B. Pant, *J. Mater. Eng. Perform.* 22 (2013) 2331–2336.
- [3] G.B. Lin, Z.D. Wang, M.K. Zhang, H. Zhang, M. Zhao, *Mater. Sci. Technol.* 27 (2011) 966–969.
- [4] C. Watanabe, R. Monzen, K. Tazaki, *J. Mater. Sci.* 43 (2008) 813–819.
- [5] X.P. Xiao, B.Q. Xiong, Q.S. Wang, G.L. Xie, L.J. Peng, G.X. Huang, *Rare Met.* 32 (2013) 144–149.
- [6] J.Y. Cheng, B. Shen, F.X. Yu, *Mater. Charact.* 81 (2013) 68–75.
- [7] P. Hanzelka, V. Musilova, T. Kralik, J. Vonka, *Cryogenics* 50 (2010) 737–742.
- [8] J.H. Su, Q.M. Dong, P. Liu, H.J. Li, B.X. Kang, *Mater. Sci. Eng. A* 392 (2005) 422–426.
- [9] S.C. Krishna, N.K. Gangwar, A.K. Jha, B. Pant, K.M. George, *J. Mater. Eng. Perform.* 23 (2014) 1458–1464.
- [10] S. Suzuki, N. Shibutani, K. Mimura, *J. Alloy. Compd.* 417 (2006) 116–120.
- [11] H. Zhang, H.G. Zhang, L.X. Li, *J. Mater. Process. Technol.* 209 (2009) 2892–2896.
- [12] Y.Q. Long, P. Liu, Y. Liu, W.M. Zhang, J.S. Pan, *Mater. Lett.* 62 (2008) 3039–3042.
- [13] J.H. Choi, *Mater. Sci. Eng. A* 550 (2012) 183–190.
- [14] L.M. Bi, P. Liu, X.H. Chen, X.K. Liu, W. Li, F.C. Ma, *Trans. Nonferrous Met. Soc. China* 23 (2013) 1342–1348.
- [15] Y. Pang, C.D. Xia, M.P. Wang, Z. Li, Z. Xiao, H.G. Wei, X.F. Sheng, Y.L. Jia, C. Chen, *J. Alloy. Compd.* 582 (2014) 786–792.
- [16] C.D. Xia, Y.L. Jia, W. Zhang, K. Zhang, Q.Y. Dong, G.Y. Xu, M. Wang, *Mater. Des.* 39 (2012) 404–409.
- [17] S.G. Mu, F.A. Guo, Y.Q. Tang, X.M. Cao, M.T. Tang, *Mater. Sci. Eng. A* 475 (2008) 235–240.
- [18] Z.Y. Pan, J.B. Chan, J.F. Li, *Trans. Nonferrous Met. Soc. China* 25 (2015) 1206–1214.
- [19] P. Liu, B.X. Kang, X.G. Cao, J.L. Huang, B. Yen, H.C. Gu, *Mater. Sci. Eng. A* 265 (1999) 262–267.
- [20] J.H. Su, P. Liu, Q.M. Dong, H.J. Li, F.Z. Ren, B.H. Tian, *J. Mater. Eng. Perform.* 16 (2007) 490–493.
- [21] D.M. Zhao, Q.M. Dong, P. Liu, B.X. Kang, J.L. Huang, Z.H. Jin, *Mater. Sci. Eng. A* 361 (2003) 93–99.
- [22] J.H. Su, P. Liu, Q.M. Dong, H.J. Li, F.Z. Ren, *J. Mater. Process. Technol.* 205 (2008) 366–369.
- [23] M. Xie, J.L. Liu, X.Y. Lu, A. Shi, Z.M. Den, H. Jang, F.Q. Zheng, *Mater. Sci. Eng. A* 305 (2001) 529–533.
- [24] F.A. Guo, C.J. Xiang, C.X. Yang, X.M. Cao, S.G. Mu, Y.Q. Tang, *Mater. Sci. Eng. B* 147 (2008) 1–6.
- [25] J.H. Su, P. Liu, H.J. Li, F.Z. Ren, Q.M. Dong, *Mater. Lett.* 61 (2007) 4963–4966.
- [26] Q. Lei, Z. Li, Z.Y. Pan, M.P. Wang, X. Zhu, C. Chen, *Trans. Nonferrous Met. Soc. China* 20 (2010) 1006–1011.